Science of the Total Environment 627 (2018) 671–680

Contents lists available at ScienceDirect

Science of the Total Environment

journal homepage: www.elsevier.com/locate/scitotenv

Spatial variation and sources of polycyclic aromatic hydrocarbons influenced by intensive land use in an urbanized river network of East China

Chunjuan Bi [a,b,*], Xueping Wang [c,1], Jinpu Jia [a,2], Zhenlou Chen [a,3]

[a] Key Laboratory of Geographic Information Science of Ministry of Education, School of Geographic Sciences, East China Normal University, Shanghai 200241, China
[b] Chongming Ecological Research Center, East China Normal University, Shanghai 200241, China
[c] Guangxi Key Laboratory of Marine Disaster in the Beibu Gulf, Qinzhou University, Qinzhou 535011, China

HIGHLIGHTS

- PAHs were analyzed in water, SPM and sediments of Shanghai river network.
- PAHs in SPM and sediments showed the highest concentrations in inner city.
- Main factors affecting the partitioning and spatial variations of PAHs were analyzed.
- Vehicle emissions in the urbanized and industrialized areas contributed strongly to PAHs.

GRAPHICAL ABSTRACT

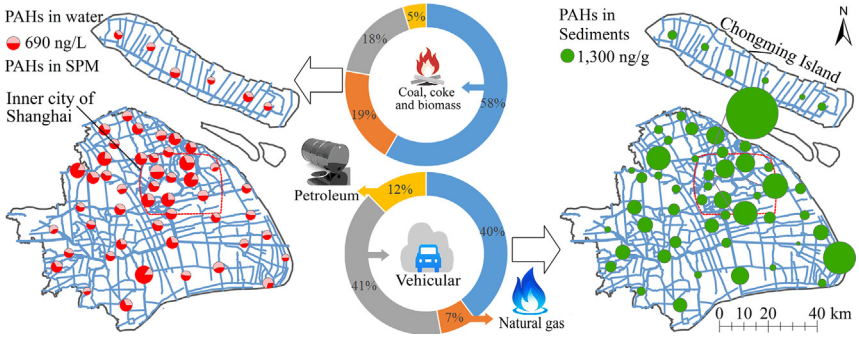

ARTICLE INFO

Article history:
Received 4 December 2017
Received in revised form 25 January 2018
Accepted 26 January 2018
Available online xxxx

Editor: Jay Gan

Keywords:
Distribution
Partitioning
Influence factor
Anthropogenic input
PMF

ABSTRACT

The concentrations and distribution of polycyclic aromatic hydrocarbons (PAHs) in urbanized river networks are strongly influenced by intensive land use, industrial activities and population density. The spatial variations and their influencing factors of 16 priority PAHs were investigated in surface water, suspended particulate matter (SPM) and sediments among areas under different intensive land uses (industrial areas, agricultural areas, inner city, suburban towns and island areas) in the Shanghai river network, East China. Source apportionment was carried out using isomer ratios of PAHs and Positive Matrix Factorization (PMF). Total concentrations of 16 PAHs ranged from 105.2 to 400.5 ng/L, 108.1 to 1058.8 ng/L and 104.4 to 19,480.0 ng/g in water, SPM and sediments, respectively. The concentrations of PAHs in SPM and sediments varied significantly among areas ($p < 0.05$), with the highest concentrations in inner city characterized by highly intensive land use and high population density. The PAH concentrations in sediments were positively correlated with those in SPM and were more strongly correlated with black carbon than with total organic carbon, indicating a stronger influence of prolonged anthropogenic contamination than the recent surface input in sediments. Biomass and coal combustion contributed strongly to total PAHs, followed by natural gas combustion in water and SPM, and vehicular emissions in

* Corresponding author at: Room 306, Building of Environmental and Resources, 500 Dongchuan Road, Minhang District, Shanghai 200241, China.
E-mail address: cjbi@geo.ecnu.edu.cn (C. Bi).
[1] Postal address: Room 301, Building of Ocean college, 12 Binhai Road, Qinnan District, Qinzhou, China, 535,011.
[2] Postal address: Room 306, Building of Environmental and Resources, 500 Dongchuan Road, Minhang District, Shanghai, China, 200,241.
[3] Postal address: Room 331, Building of Environmental and Resources, 500 Dongchuan Road, Minhang District, Shanghai, China, 200,241.

https://doi.org/10.1016/j.scitotenv.2018.01.272

sediments. Vehicular emissions were the strongest contributors in SPM and sediments of the inner city, indicating the strong influence of vehicular transportation to PAHs pollution in the urbanized river network.

1. Introduction

PAHs are ubiquitous environmental contaminants and have received considerable attention because of their toxic, mutagenic and carcinogenic characteristics (Long et al., 1995; Menzie and Potokib, 1992). Anthropogenic PAH sources have been identified to mainly originate from vehicular emissions, industrial activities, domestic heating, waste incineration, petroleum spills, biomass and coal combustion (Guo et al., 2009; Harrison et al., 1996; Simcik et al., 1999; Zhang et al., 2017). The PAHs generated from these anthropogenic sources and natural processes such as volcanoes and forest fires can be transported to surface water through atmospheric deposition, road runoff, spillage of petroleum products and wastewater discharges (Herngren et al., 2010; Uher et al., 2016). As a result of their hydrophobic characteristics, PAHs in aquatic environments tend to become associated with suspended particles and are subsequently deposited to the sediment layers.

Intensive industries and urbanization activities have an important influence on the spatial distribution of PAHs in the aquatic system (Chen et al., 2007; Ligaray et al., 2016; Timoney and Lee, 2011). Sediment PAH concentrations in the Athabasca River Delta were related to industrial activities (Timoney and Lee, 2011). Urban areas have the highest PAH loadings compared to rural areas (Chen et al., 2007; Ligaray et al., 2016). Timoney and Lee (2011) found no significant correlations between river discharge variables and sediment PAH concentrations. Intensive urban use was identified as the most important factor influencing PAH distribution in river sediments, which not only led to highly PAH-polluted river sediments, but also resulted in significant fluctuation of PAH levels among locations (Liu, A. et al., 2017). Dissolved and labile phases of PAHs were the phases most related to the watershed population density, whereas particulate PAHs were more related to local pressure (Uher et al., 2016).

Numerous studies have reported the levels, spatial and temporal variations, partitioning characteristics, sources and ecological risks of PAHs in river systems (Montuori et al., 2016; Sarria-Villa et al., 2016; Zhang et al., 2017). Almost all related research has focused mainly on individual rivers or river sections; however, in some coastal regions, several rivers are interconnected with each other and form river networks. To date, few studies have been conducted on PAH pollution in these river networks (Liu et al., 2016). Given their location and interconnected nature, these river networks would be more influenced by intensive urban land use, industries and population density.

The Shanghai river network is a highly urbanized and industrialized region in China and is a typical river network with weak hydrodynamic conditions. The distribution of PAHs in three hierarchical rivers in this region and sources of PAHs in surface sediments of the Huangpu River were reported (Liu et al., 2009; Liu et al., 2016). The aims of this study were to investigate the concentrations and spatial variation of PAHs in water, SPM and sediments among different intensive land uses and to analyze the main factors affecting the partitioning and distribution of PAHs in multiple phases of the Shanghai river network to ultimately identify and quantitatively assess source contributions to PAHs. The results of this research will be useful for alleviating PAH contamination in urbanized river networks worldwide.

2. Materials and methods

2.1. Study area and samples collection

The study area is located in Shanghai (30°40′–31°53′ N, 120°52′–122°12′E), which is one of the largest and most important industrial cities in China, and sits on the Yangtze Estuary of East China. Shanghai belongs to the northern subtropical monsoon climate zone, with an annual average precipitation of 1435.8 mm, an annual rainy days of 151 days, and an annual mean temperature of 17.1 °C in 2012 (SMSB, 2013). The main land Shanghai involves a soft deltaic deposit with some isolated outcrops of bedrock. Under the upper clayey soil, there is a sand layer, which is a phreatic aquifer, where the groundwater level is 0.5–2.5 m below the surface (Shen et al., 2014). There are about 33,127 rivers or creeks in Shanghai, with a length of ~24,915 km and total water area of ~642.7 km^2 (SMWAB, 2016). These rivers are interconnected with each other, producing a river network. Huangpu River is the dominant river in this river network system and the last tributary of the Yangtze River before discharge to the ocean. Except for the Huangpu River, most of the rivers have been cut off by flood gates in this river network system, which results in weak hydrodynamic conditions. The length of drainage sewer pipes and the number of pumping stations were 18,191 km and 183 in 2012 (SMSB, 2013). The increased surface runoff due to land surface modification during urbanization has aggravated the burden of drainage network.

The population density in Shanghai reached 3754 persons/km^2 in 2012, and the maximum population density in the inner city was up to 36,014 persons/km^2 (SMSB, 2013). There are 104 small towns outside the inner city areas, the total area of which accounts for 87.08% of the total area of Shanghai, and the total population of the township accounts for 50.60% of the total resident population in Shanghai (Liu, H. et al., 2017).The average daily energy consumption in Shanghai in 2012 were 12.73×10^7 kg for coal, 1.84×10^7 kg for coke, 1.75×10^7 kg for fuel oil, 1.56×10^7 kg for diesel oil, 1.42×10^7 kg for gasoline, 1.10×10^7 kg for kerosene, 18 million m^3 for diesel oil and 371 million kwh for electricity (SMSB, 2013). Six key industries including electronic information product manufacturing, automobile manufacturing, petrochemical and fine chemical products manufacturing, fine steel manufacturing, equipment complex manufacturing and bio-medicine manufacturing contributed 66.0% to the total gross output value of industry in Shanghai in 2012 (SMSB, 2013). The total sown area of the crops was 3.9×10^5 hm^2, of which the grain crops and the economic crops contributed 48.1% and 51.9% respectively (SMSB, 2013).

According to the principle of gridded stationing, 53 sampling sites were selected for sample collection from areas under the following intensive land uses: inner city ($n = 11$), industrial areas ($n = 11$), agricultural areas ($n = 15$), suburban towns ($n = 10$) and island areas on Chongming Island ($n = 6$) (Fig.1). Detailed description of sampling areas was listed in Table 1. Chongming Island, with the population density of 590 persons/km^2 (SMSB, 2013), is located in the Yangtze estuary and aims to develop ecological agriculture. The rivers on the island are connected to the Yangtze River, so the river network on Chongming Island is separated into island areas. Sampling sites were selected from straight flowing river section in the Sampling grid. Sewage outlets and new dredged river sections without sediments were avoided.

Surface water, SPM and surface sediment samples were collected in April 2012. Samples were collected in the middle of the river cross section by means of a bridge or a boat. Bipartite samples of surface water (5–15 cm depth) were collected using a plexiglass sampler and stored in 1 L clean brown glass bottles; surface sediments (0–15 cm depth) were sampled using the Ekman-Birge bottom sampler (HYDRO-BIOS, Germany) and stored in sealed polyethylene bags. Both water and sediment samples were directly transported to the laboratory after sampling and stored at 4 °C and −18 °C, respectively. A global positioning system (GPS) was used to locate the sampling sites. Temperature, pH and dissolved oxygen (DO) contents of the river water were measured

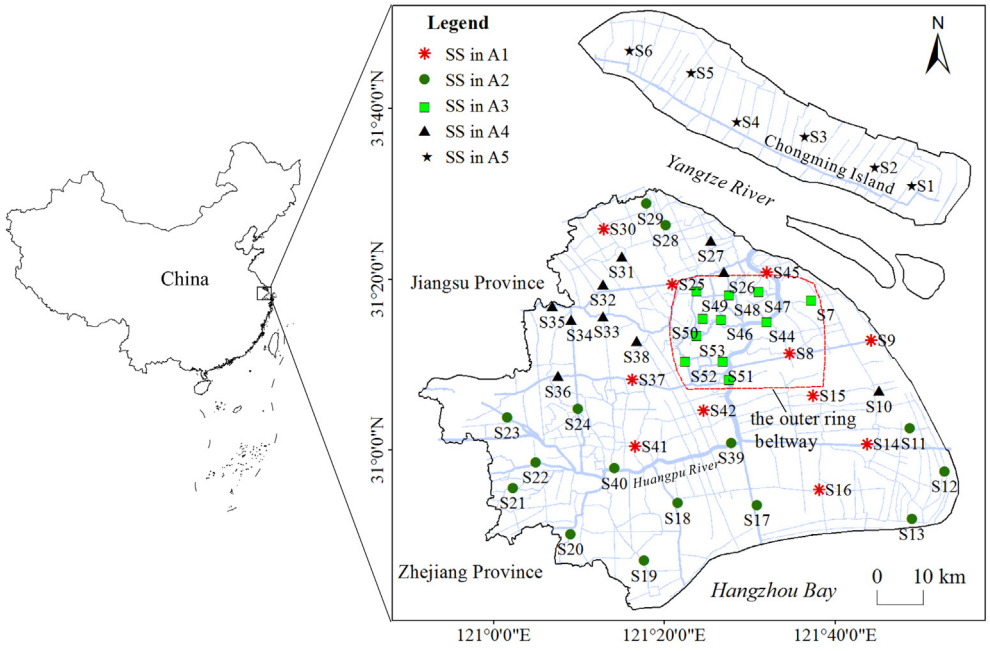

Fig. 1. Location of sampling sites (SS) in Shanghai river network among areas under different intensive land uses. A1, industrial areas; A2, agricultural areas; A3, inner city; A4, suburban towns; A5, island areas.

in situ using a portable pH meter (IQ150, USA) and a dissolved oxygen meter (YSI55, USA), respectively.

2.2. Sample preparation and analysis

Water samples were filtrated by 0.7 μm pore size glass fiber filters (Waterman, UK), which were combusted at 450 °C prior to use. Filtrates were extracted using solid phase extraction (Supelco, USA). Before the extraction, the Oasis HLB columns (Waters, USA) were activated by 5 mL of n-hexane, dichloromethane, methanol and ultra-pure water, successively. The filtrate was then percolated at 5 mL/min and the columns were eluted by 10 mL mixture solvent of dichloromethane and n-hexane (3:7, v/v) after extraction. The elution was dried by anhydrous Na_2SO_4, transferred with n-hexane and concentrated to 0.9 mL using DryVap automatic concentrator (Horizon, USA).

The SPM samples separated by GFF and sediments were freeze-dried using a freeze dryer (Christ, Germany). After drying, total suspended solids (TSS) contents of the river water were calculated according to the lost weight of the GFF. The SPM and sieved sediment samples (60 meshes) were extracted using accelerated solvent extraction (ASE300, Dionex, USA). After mixing with alumina and activated copper, solid samples were extracted using acetone and dichloromethane (1:1, v/v) under 1500 psi at 100 °C for 4 cycles of static extraction. Extraction was then purified by a silica-alumina column packed with anhydrous sodium sulfate, alumina, silica and quartz sand from top to bottom (silica activated at 130 °C for >16 h; other reagents dried at 450 °C for 4 h). The column was firstly washed with n-hexane before purification and then eluted with 70 mL mixed solvent of dichloromethane and n-hexane (3:7, v/v) at 2–3 mL/min. The elution was then transferred with n-hexane and concentrated to 0.9 mL using DryVap automatic concentrator (Horizon, USA). Finally, all the concentrated solution of water, SPM and sediments were fixed to 1 mL after 0.1 mL decachlorobiphenyl (Supelco, USA) was added to the solution.

The PAH concentrations in samples were measured using GC/MS (Agilent 7890GC/5975 MSD, USA) in EI mode equipped with a HP-5MS capillary column (30.0 m × 0.25 mm × 0.25 μm) and a CTC automatic sampling injector (Switzerland) with helium as carrier gas at a 1 mL/min flow rate. The oven temperature was held at 80 °C for 2 min, increased to 235 °C at a rate of 10 °C/min and continually ramped at 4 °C/min to 300 °C, then held for 4 min. The transfer line and ion trap manifold were set at 280 °C and 230 °C, respectively. The following 16 PAHs prioritized by the US EPA were analyzed: naphthalene (Nap), acenaphthylene (Acy), fluorene (Flu), phenanthrene (Phe), acenaphthene (Ace), anthracene (Ant), fluoranthene (Fla), pyrene (Pyr), benzo[*a*]anthracene (BaA), chrysene (Chr), benzo[*b*]fluoranthene (BbF), benzo[*k*]fluoranthene (BkF), benzo[*a*]pyrene (BaP), indeno[1,2,3-c,d]pyrene (IcdP), benzo[*g,h,i*]perylene (BghiP) and dibenzo[*a,h*]anthracene (DahA). All solvents used for sample processing such as n-hexane, dichloromethane, methanol and acetone were pesticide analysis grade from Merk (USA). The PAH concentrations of SPM and sediment samples were based on dry weight.

Dissolved organic carbon (DOC) in the filtrate was detected by a Liqui TOC II analyzer (Germany). The total organic carbon (TOC) in sediments was measured using the potassium dichromate oxidation-external heating method (Nelson and Sommers, 1982). Black carbon (BC) in sediments was quantified using an elemental analyzer (Elementar Vario Micro, Germany) after removal of organic carbon by thermal oxidation and inorganic carbon by acidification (Gelinas et al., 2001; Gustafsson

Table 1
Sampling sites partitions of Shanghai river network.

Sampling areas	Sample number	Sampling sites	Description of sampling areas
Inner city	11	S7, S43, S44, S46, S47, S48, S49, S50, S51, S52, S53	Within the outer ring beltway, mostly commercial areas, public facilities, and urban residences
Industrial areas	11	S8, S9, S14, S15, S16, S25, S30, S37, S41, S42, S45	In the zone of industrial parks in Shanghai
Agricultural areas	15	S11, S12, S13, S17, S18, S19, S20, S21, S22, S23, S24, S28, S29, S39, S40	Suburban farmland growing rice and vegetables
Suburban towns	10	S10, S26, S27, S31, S32, S33, S34, S35, S36, S38	Mainly located in the residences of suburban town centers
Island areas	6	S1, S2, S3, S4, S5, S6	On Chongming island, directly connected to the Yangtze River

et al., 1997). The grain size of sediment was measured using a laser diffraction particle analyzer (LS13320, USA) following ultrasonic particle dispersion with $(NaPO_3)_6$ solution (Ding et al., 1998).

2.3. Quality assurance and quality control

The concentrations of PAHs in this study were quantified by internal standard method. Deuterated PAHs of 0.5 mg/L (d_8-napthalene, d_{10}-acenaphthene, d_{10}-anthracene, d_{12}-chrysene and d_{12}-perylene) were used as the surrogate standard solution (Supelco, USA). In addition, blank samples and parallel samples were tested every ten samples. The linearity coefficients (R^2) of standard curve were 0.9972–0.9999. Target compounds were under limit of detection in blanks. The recoveries of deuterated PAHs were above 68.5%–74.0% in water and 67.0%–83.5% in SPM and sediments. The limit of detection (LOD, S/N = 3) and the limit of quantification (LOQ, S/N = 10) were 0.3–1.3 ng/L and 1–5 ng/L respectively, while in SPM and sediments, the LOD and LQD were 0.03–0.5 ng/g and 0.1–2 ng/g respectively. The repeatability (r) and reproducibility (R) through the detection of one sample by two technicians of the same laboratory and two laboratories for seven times were 3.3%–8.7% and 5.7%–10.2%, respectively.

2.4. Data analysis

Isomer ratios of PAHs were used to qualitative analysis the major sources of PAHs in water, SPM and sediments in this study. Among the possible isomer ratios, Fla./(Fla + Pyr), Ant/(Ant+Phe) and BaA/(BaA + Chr) are most widely used for source identification of PAHs in river water and sediments (Chen et al., 2007; Montuori et al., 2016; Zhang et al., 2017). For Ant/(Ant+Phe), ratios >0.1 and <0.1 indicate the pyrogenic origin and petrogenic origin of PAHs, respectively (Yunker et al., 2002). For Fla/(Fla + Pyr), high ratios (>0.5) indicate biomass and coal combustion, ratios between 0.4 and 0.5 suggest petroleum combustion, while ratios <0.4 are characteristic of petroleum (Yunker et al., 2002). For BaA/(BaA + Chr), ratios >0.35 and <0.35 indicate biomass & coal combustion and petroleum combustion, respectively (Yunker et al., 2002).

The PMF model has been widely used to calculate the profile and contribution of sources in the aquatic environment (Wang et al., 2013; Yu et al., 2015). This model constrains the solutions with non-negative values and decomposes receptors by factor contribution (g_{ik}), factor profile (f_{kj}) and residual matrix (e_{ij}) as follows:

$$X_{ij} = \sum_{k=1}^{p} g_{ik} f_{kj} + e_{ij} \quad (1)$$

where X_{ij} is the j species concentration measured in sample i, g_{ik} is the contribution of factor k to sample i, p is the factor number, f_{kj} is the fraction of species j in factor profile k and e_{ij} is the residual for each sample/species.

Next, g_{ik} and f_{kj} are derived by the PMF model minimizing the objective function Q:

$$Q = \sum_{i=1}^{n} \sum_{j=1}^{m} \left(\frac{e_{ij}}{u_{ij}} \right)^2 \quad (2)$$

where u_{ij} is the uncertainty for each sample/species, m is the number of species and n is the number of samples. The uncertainties for each sample were calculated by using relative uncertainty of PAHs concentrations and LOD. When the sample concentration was ≤LOD, the uncertainty u was calculated as:

$$u = \frac{5}{6} \times LOD \quad (3)$$

while when the sample concentration was >LOD, u was calculated as:

$$u = \sqrt{(\mathrm{RSD} \times concentration)^2 + (0.5 \times \mathrm{LOD})^2} \quad (4)$$

where RSD is the error faction calculated by the real concentrations of each samples. When the concentration of PAHs in any samples was not determined (ND), it was calculated as the half of LOD. The EPA PMF 5.0 model was used in this study (Norris and Duvall, 2014).

The data were statistically analyzed using SPSS ver. 23. A variance analysis ($p < 0.05$) of total PAHs among different areas was performed using a one-way ANOVA test. The correlation analysis was conducted by a Pearson correlation, and the level of significance was set at $p < 0.05$ (two-tailed).

3. Results and discussion

3.1. Occurrence of PAHs in river water, SPM and sediments

The concentrations of dissolved PAHs ranged from 105.2 to 400.5 ng/L with a mean value of 178.7 ng/L in surface water of the Shanghai river network (Table 2), which were higher than those from other areas such as 1.8–607.5 ng/L in the Tiber River and estuary, Italy (Montuori et al., 2016), and 62.9–144.7 ng/L in the Mississippi River, USA (Zhang et al., 2007), but much lower than those from rivers and estuaries elsewhere such as 70.3–1844.4 ng/L in the Qiantang River (Chen et al., 2007), 548.0–2598.0 ng/L in the upper reaches of the Yellow River (Zhao et al., 2015), 71.1–4255.4 ng/L in the Daliao River estuary of China (Zheng et al., 2016), and 52.1–12,888.2 ng/L in the Cauca River, Colombia (Sarria-Villa et al., 2016). The concentrations of total PAHs in SPM ranged from 108.1 to 1058.8 ng/L with an average value of 299.1 ng/L (Table 2), which were higher than those from other areas such as 4.5–473.4 ng/L in the Tiber River and estuary, Italy (Montuori et al., 2016), but much lower than those from other rivers and estuaries such as 1969.9–11,612.2 ng/L in the Daliao River estuary of China (Zheng et al., 2016) and 1300–7000 ng/L in the Mississippi River, USA (Mitra and Bianchi, 2003). The concentrations of particulate PAHs in the 73.6% sampling sites were higher than those of dissolved PAHs based on volume concentration, which was mainly related to TSS contents in the river water.

All 16 PAHs were identified in sediment samples. The concentrations of total PAHs in sediments varied from 104.4 to 19,480.0 ng/g with an average of 1562.2 ng/g (Table 2), which were lower than those in SPM. These values were higher than those of the rivers in the Qiantang River (91.3–614.4 ng/g) (Chen et al., 2007), the Yellow River, China (181.0–1583.0 ng/g) (Zhao et al., 2015), the Cauca River, Colombia (ND–3739.0 ng/g) (Sarria-Villa et al., 2016), and the Tiber River and estuary, Italy (36.2–545.6 ng/g) (Montuori et al., 2016), and far below those of the Daliao River and estuary in China (374.8–11,588.8 ng/g) (Zheng et al., 2016), and the Ammer River in Germany (112–22,900 ng/g) (Liu et al., 2013).

The results showed that the levels of PAHs in water, SPM and sediments of the Shanghai river network were low to moderate in comparison with other rivers abroad the world. Effect range low (ERL) and effect range median (ERM) were used as guidelines to further assess the sediment quality of PAHs. These metrics provide useful assistance in efforts to protect the aquatic environment (Chen et al., 2007). The mean concentration of total PAHs was much lower than the ERL value and most of the 16 PAHs were lower than their respective ERL values except for Flu and Ant, which were far below their ERM values (Table 2). The highest concentrations of the 16 PAHs were between their ERL and ERM values except for Acy, which was lower than the ERL value (Table 2). These results suggested that PAH concentrations in most of the sediments could not be associated with adverse effects, but occasional biologically toxic effects may occur in some river sediments.

Table 2
Statistics of PAHs concentrations in surface water, SPM and sediments of the Shanghai river network.

PAH compounds	Water (ng/L)		SPM (ng/L)		Sediments (ng/g, dw)		Guidelines[c]	
	Mean ± SD[a]	Range	Mean ± SD	Range	Mean ± SD	Range	ERL	ERM
Nap	12.9 ± 24.5	1.9–181.7	13. 7 ± 6.5	2.6–38.6	40.5 ± 44.5	0.2–171.3	160	2100
Acy	6.7 ± 0.6	5.9–8.6	7.9 ± 8.0	ND[b]–42.4	5.6 ± 6.1	0.4–29.3	44	640
Ace	9.2 ± 1.9	7.6–17.4	9.7 ± 1.6	7.6–13.6	19.1 ± 29.0	0.1–157.3	16	500
Flu	13.5 ± 3.4	10.2–28.5	16.9 ± 5.9	10.2–36.6	40.3 ± 67.1	1.9–416.9	19	540
Phe	20.0 ± 5.2	15.2–46.9	28.8 ± 10.7	13.9–70.1	197.6 ± 430.5	7.2–2929.6	240	1500
Ant	11.3 ± 1.3	9.8–17.4	72.7 ± 130.8	12.9–800.4	178.3 ± 432.7	1.6–2937.5	85.3	1100
Fla	14.2 ± 2.6	11.0–24.0	17.8 ± 6.8	10.8–42.2	208.3 ± 442.8	1.23–2823.5	600	5100
Pyr	14.6 ± 5.2	10.8–48.6	14.9 ± 4.5	ND–26.3	200.5 ± 409.7	8.1–2800.6	665	2600
BaA	17.6 ± 7.0	ND–24.8	14.9 ± 10.5	ND–30.7	93.4 ± 191.5	2.8–1314.5	261	1600
Chr	12.7 ± 5.9	ND–19.8	12.8 ± 9.0	ND–37.2	103.2 ± 194.2	2.9–1276.8	384	2800
BbF	11.7 ± 9.6	ND–22.9	18.2 ± 11.4	ND–49.7	100.6 ± 176.0	9.9–1108.9		
BkF	8.4 ± 7.7	ND–18.5	13.0 ± 9.5	ND–38.2	82.4 ± 142.7	2.9–879.3		
BaP	20.8 ± 1.3	18.9–26.0	18.7 ± 10.8	ND–50.7	114.7 ± 227.3	4.4–1524.2	430	1600
IcdP	2.0 ± 6.4	ND–23.2	5. 6 ± 10.5	ND–34.9	81.4 ± 95.5	7.9–417.2		
DahA	0.9 ± 4.5	ND–24.4	26.9 ± 22.9	ND–142.7	17.8 ± 16.0	9.1–103.7	63.4	260
BghiP	2.3 ± 5.9	ND–19.8	6.7 ± 9.6	ND–29.3	89.1 ± 138.9	10.4–885.0		
$\sum_{16}$PAHs	178.7 ± 52.8	105.2–400.5	299.1 ± 181.3	108.1–1058.8	1562.2 ± 2843.4	104.4–19,480.0	4022[d]	44792[d]

[a] Standard deviation.
[b] Not determined.
[c] Effects-based guideline values (Long et al., 1995).
[d] Total values of 13 PAHs.

The compositions of PAHs in multiple media of the Shanghai river network (Fig. 2) showed that high molecular weight (HMW) PAHs (≥4 rings) had a higher concentration in sediments than low molecular weight (LMW) PAH species (<4 rings), accounting for 71.7% and 28.3% of total PAHs, respectively. The HMW PAHs also contributed >50% to total PAHs in water and SPM. The concentrations of LMW PAHs in water and SPM were higher than those in sediments, suggesting high inputs from recent processes in river water, such as atmospheric deposition and urban surface runoff (Zhang et al., 2017).

3.2. Spatial variations and partitioning of PAHs in rivers

3.2.1. Spatial variations of PAHs influenced by intensive land use

For water samples, the total PAH concentration fluctuation was relatively small among different areas ($p > 0.05$) (Fig. 3a). However, the total PAH concentrations in SPM varied significantly ($p < 0.05$) with the highest concentrations in the inner city, followed by suburban towns, industrial areas, agricultural areas and island areas (Fig. 3b). Sediment total PAH concentrations also varied greatly between different areas ($p < 0.05$); the highest concentrations were found in the inner city and lowest concentrations in island areas (Fig. 3c). It is noteworthy that the maximum value of PAHs (19,480.0 ng/g) observed in the inner city was much higher than those at other sites and was found at Site S49, which is a black and odorous river. Samples from site S47, S48 and S50, which located in black and odorous river sections in the inner city, also showed high concentrations of PAHs in sediments. High PAH concentrations in an urban black and odorous river in Shenzhen of China were also reported in Liu, T. et al. (2017). Intensive anthropogenic activities within urban areas causes increased loading of both PAHs and other organic pollutants.

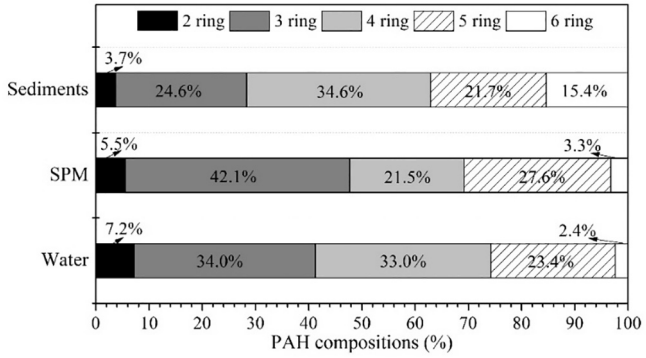

Fig. 2. Compositions of 2–6-ring PAHs in surface water, SPM and sediments of the Shanghai river network.

As a result of the weak hydrodynamic conditions in the studied areas, pollutants are not easily diffused and typically accumulate in rivers. Thus, PAHs in river water and sediments showed high concentrations in areas with highly intensive land use and high population density, which was consistent with the findings of Chen et al. (2007) and Ligaray et al. (2016). The intensive urban use area was characterized by various anthropogenic activities such as fossil fuel combustion and industrial activities, which not only led to highly PAH-polluted river sediments, but also led to fluctuating PAH concentrations among locations (Fig. 3) (Liu, A. et al., 2017). The PAHs in SPM and sediments of the Shanghai river network showed significant variation among the different areas, suggesting particles and sediments were strongly related to the local influence of anthropogenic activities. A similar result was reported by Uher et al. (2016), who found that dissolved and labile phases of PAHs were strongly related to the population density of the watershed, whereas particles were strongly related to local pressure, e.g. the presence of a road next to the deployment site.

3.2.2. Partitioning of PAHs in rivers

To better understand the distribution and transport of PAHs in the Shanghai river network, the partition coefficient (K_p) (L/g) was calculated and defined as the ratio of the concentrations of PAHs associated with SPM (ng/g, dw) to that in the dissolved phase (ng/L). The K_p values of total PAHs ranged from 8.5 to 168.0 L/g, with a mean value of 47.8 L/g. Compared with the Yangtze estuarine and nearby coastal area (0.5–10.2 L/g) (Ou et al., 2009), there were much higher K_p values in the Shanghai river network, suggesting that PAHs tended to bind with SPM under the relatively weak dynamic conditions. The mean K_p values in the inner city were much higher (65.7 L/g) than in other areas (35.1–47.9 L/g), indicating that highly intensive urban use also influenced the PAH partitioning in water and SPM. The PAHs bound to particles on the urban surface would directly enter the rivers through surface runoff and lead to the high K_p in the inner city area. The K_p values of PAHs in most surface runoff samples from residential road, parking lot, junction area, roof and main road varied between 50 and 1000 L/g (Han et al., 2013). Further, the K_p values of PAHs in the surface runoff from urban main roads could be as high as 2500 L/g (Han et al., 2012).

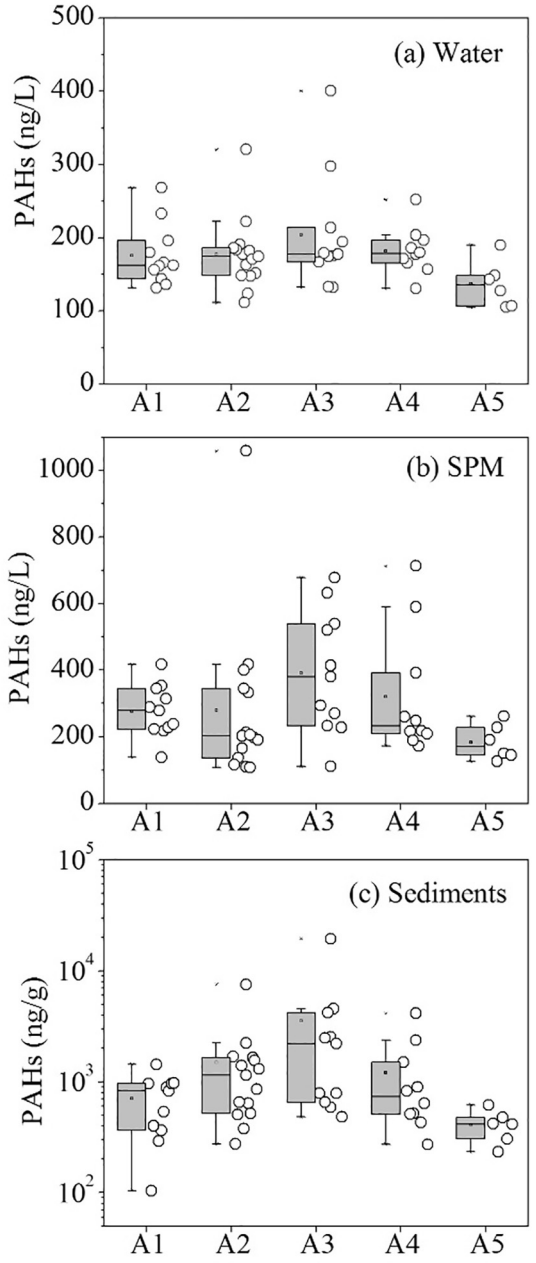

Fig. 3. Spatial variations of PAHs in surface water, SPM and sediments of the Shanghai river network. A1, industrial areas; A2, agricultural areas; A3, inner city; A4, suburban towns; A5, island areas.

3.3. Factors influencing the spatial variations of PAHs

The environmental behavior and fate of PAHs was generally believed to be ultimately determined by the physico-chemical properties of each PAH, as well as those of the water and sediment (Liu et al., 2013; Montuori et al., 2016; Zhang et al., 2017). The PAH concentrations in water of the Shanghai river network showed no correlation with DO, pH and DOC contents ($p > 0.05$), whereas the total PAHs in SPM were negatively correlated with DO and pH of the river water (Fig. 4a, b). The DO is an indicator reflecting the water quality and would decrease under a large amount of oxygen-consuming organic pollutants being discharged into the rivers. The negative correlation between PAHs and DO further confirmed that PAHs bound to particles would directly enter the rivers together with other organic pollutants. Partitioning of PAHs in water and particles could be influenced by pH, but the negative correlation between particulate PAHs and pH in this study might be more related to the pollutant input from surface runoff. The PAH concentrations in urban road runoff varied between 4.9 and 1558.0 ng/L and between 635.4 and 16,624.0 ng/L in water and SPM, respectively (Han et al., 2012). Moreover, values as high as 1862.2 ng/L were observed at the runoff confluence before discharge to the river during rain events, with a runoff pH range of 6.5–8.7 (Han et al., 2013). A large amount of surface runoff input would lead to relatively high particulate PAH concentrations in urban rivers.

The K_p values of PAHs between river water and SPM were negatively correlated with TSS contents (Fig. 4c), which was consistent with the results of Luo et al. (2008). This particle concentration effect may occur because the input of large amount of DOC derived from surface runoff led to the desorption of particulate PAHs. Furthermore, there was a negative correlation between clay contents and TSS ($r = -0.47$, $p < 0.01$). When the TSS is low, the fine soot-like particles can bind more PAHs, resulting in high K_p values (Luo et al., 2008).

The PAH concentrations in sediments were lower than those in SPM, and there was a significant positive correlation between them at all sites except S49 (Fig. 4d). This suggests that the contamination of PAHs in the Shanghai river network might be caused by fresh input of PAHs (Montuori et al., 2016), and PAHs in sediments were mainly dominated by the deposition of SPM. It has been mentioned before that Site S49 was located in a black and odorous river of inner city and had the maximum PAH value of 19,480.0 ng/g. When this sample was masked, PAH concentrations showed a positive correlation with TOC contents in sediments (Fig. 4e). If this sample was unmasked, PAH concentrations showed a much higher positive correlation with BC contents in sediments (Fig. 4f). Clay percentages of sediments were not significantly correlated with PAHs ($p > 0.05$).

Correlations of PAH concentrations with TOC contents in the Shanghai river network might indicate co-emission of PAHs and TOC, and the elevated BC fractions in sedimentary TOC and PAHs showed a prolonged anthropogenic influence (Liu et al., 2013). Therefore, PAHs in surface sediments of the Shanghai river network were more influenced by prolonged anthropogenic input than by recent surface runoff, especially in the black and odorous river of the inner city.

3.4. Source apportionment of PAHs

3.4.1. Isomer ratios of PAHs in water, SPM and sediments

Diagnostic ratios of PAHs represent one of the most widely used tools of PAH source analysis because of the relatively stable feature of isomers in the environment (Kanzari et al., 2014; Liu et al., 2013; Yunker et al., 2002). The isomer ratios reflected a dominant contribution of biomass and coal combustion input of PAHs to the Shanghai river network (Fig. 5). In detail, mean Ant/(Ant+Phe) ratios in water, SPM and sediments were 0.37, 0.54 and 0.43, respectively, and the ratios in most of the samples were >0.1, which indicated the pyrogenic origin of PAHs (Yunker et al., 2002). The high percentages of Fla./(Fla + Pyr) ratios >0.5 in water (60.4%), SPM (94.2%) and sediments (86.8%) indicated the prevailing impact of biomass and coal combustion. The percentages of 0.4 < ratios <0.5 in river water, SPM and sediments were 37.7%, 3.9% and 3.8%, respectively, indicating that petroleum combustion from traffic emissions was also an important source of PAHs, especially in river water. A BaA/(BaA + Chr) ratio > 0.35 was found in water, SPM and most sediment samples, indicating that combustion of biomass and coal were major sources of PAHs in the river network (Yunker et al., 2002).

3.4.2. PMF results for PAHs in water, SPM and sediments

The PMF model was run in the robust mode and different runs were performed to improve results by decreasing the S/N ratio from "strong" to "weak". The Q_{robust} values were approximately equivalent to the $Q_{theoretical}$ values, and the use of five factors for water and six factors for SPM and sediments provided a good fit with R^2 values for total

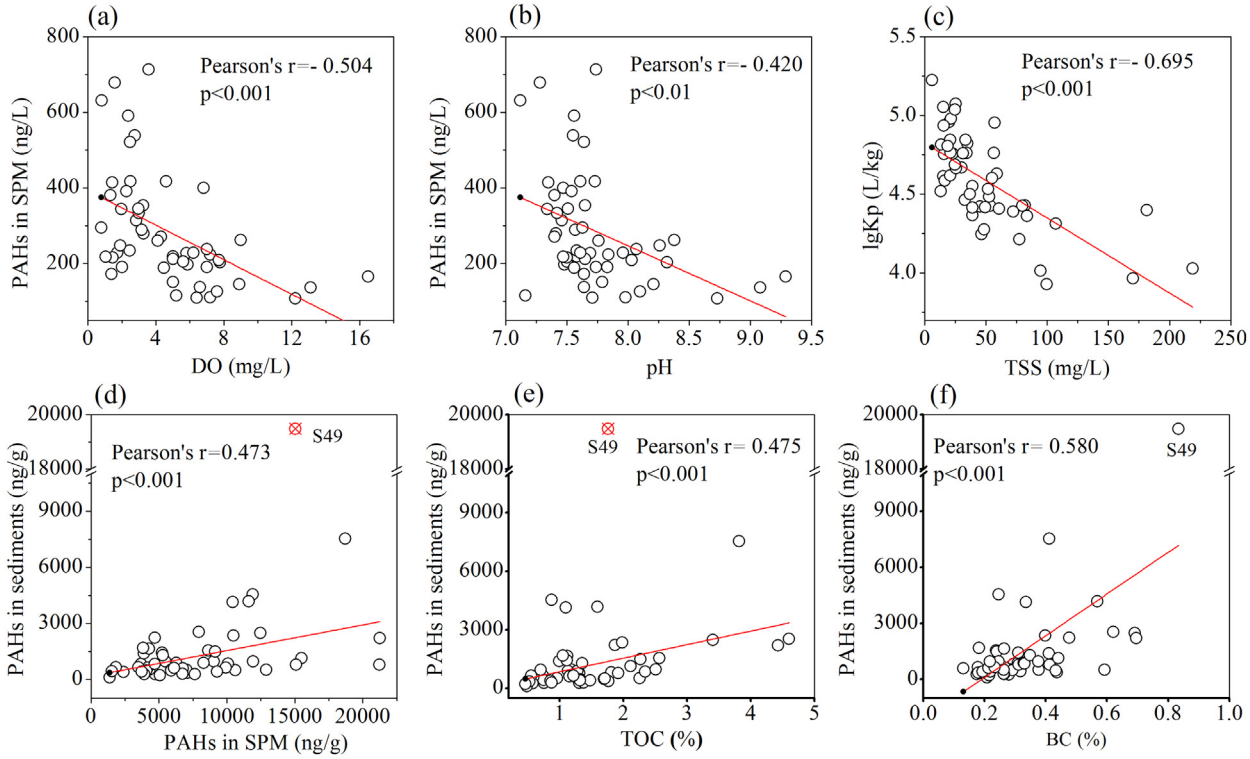

Fig. 4. Correlations between PAH concentrations and physio-chemical factors in sediments and SPM of the Shanghai river network.

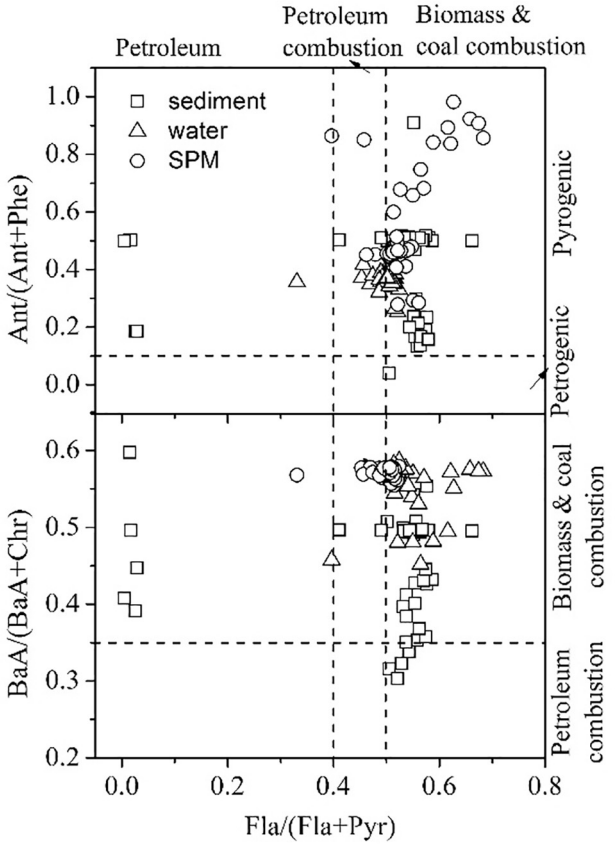

Fig. 5. Cross plots for the isomeric ratios in surface water, SPM and sediments of the Shanghai river network.

PAHs of 0.928, 0.993 and 0.999 for water, SPM and sediments, respectively.

Five source factors in the water and six factors in SPM and sediments were extracted by the PMF model (Fig. 6). In river water (Fig. 6a), Factor 1 (F1) was dominated by Flu, Phe and BkF, and moderately weighted by Ace and Ant, indicating a coal combustion and coke production source (Simcik et al., 1999; Wang et al., 2013; Zhu et al., 2001). Factor 2 (F2) was highly loaded on Pyr, Fla. and Acy with moderate loadings from Ace and Ant. Pyr, Fla. and Ant were related with wood combustion (Harrison et al., 1996), and Acy was used to indicate wood/firewood combustion (Lee et al., 2005). Thus, F2 reflected the biomass combustion source. Factor 3 (F3) was predominantly loaded on Nap, which is representative of petroleum spills originating from gasoline and diesel fuel leakage (Marr et al., 1999). Factor 4 (F4) was dominated by BbF, BaP, IcdP, DahA and BghiP, which included only high molecular weight PAHs (4–6 rings) and were related to vehicular emissions (Harrison et al., 1996; Yu et al., 2015). Factor 5 (F5) was highly loaded with BaA and Chr and could be assigned to represent natural gas combustion (Simcik et al., 1999). According to above source fingerprint of each PAH, biomass combustion, petroleum spills, vehicular emissions and natural gas combustion were identified to be the sources of F1, F2, F3 and F5 in SPM, respectively (Fig. 6b). Natural gas combustion, petroleum spills, vehicular emissions and biomass combustion were the sources of F1, F3, F4 and F5 in sediments, respectively (Fig. 6c). Factor 6 (F6) in SPM was highly dominated by BkF (Fig. 6b) and F6 in sediments was predominantly loaded on BkF and BbF with moderate loadings from Pyr, BaA, Chr and BaP (Fig. 6c). BkF, Chr, BaP and IcdP were identified as emissions from coke working in a coke plant (Zhu et al., 2001). Thus, the coke production source was separated from the coal combustion source in SPM and sediments.

The source contribution of total PAHs of each factor was also estimated by the PMF model. The coal or coke combustion, biomass combustion, natural gas combustion, petroleum spills and vehicular emission sources represented 49.9%, 12.0%, 16.7%, 4.9% and 16.5% for water, respectively; 46.1%, 11.6%, 20.6%, 5.3% and 16.4% for SPM, respectively; and 40.2%, 4.2%, 10.9%, 8.7% and 36.0% for sediments,

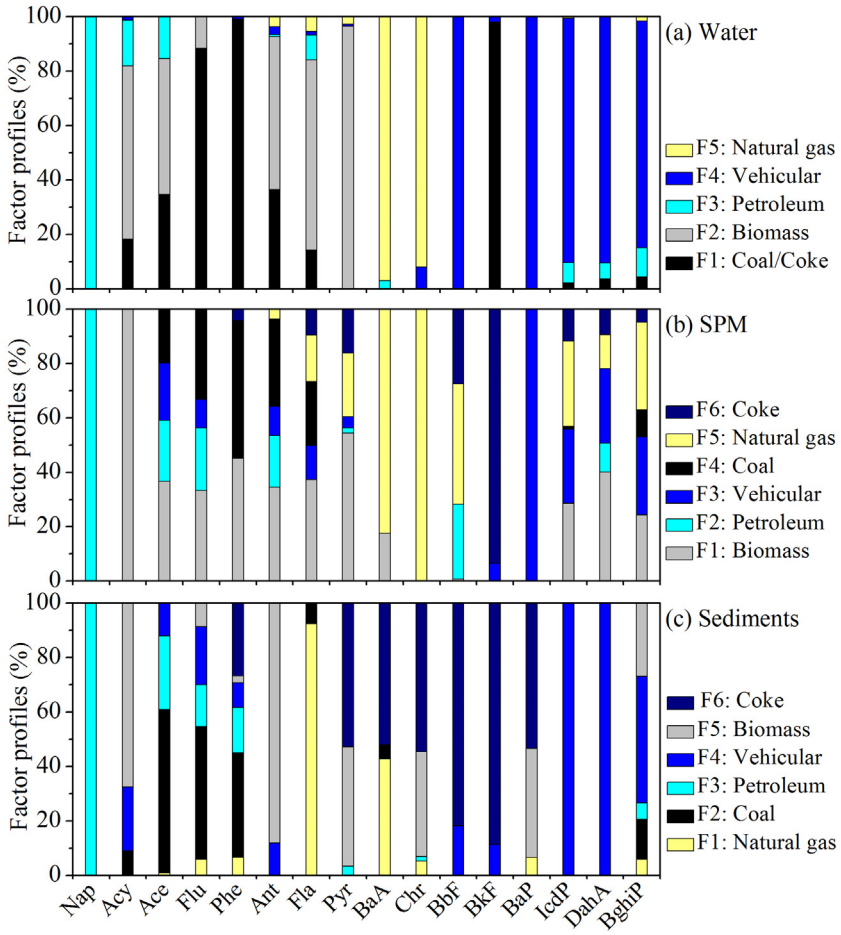

Fig. 6. Fingerprints of 16 PAHs by PMF in surface water, SPM and sediments of the Shanghai river network.

respectively. Biomass and coal combustion contributed largely to total PAHs, followed by petroleum combustion (sum of vehicular emissions and natural gas combustion), which was consistent with the result of diagnostic ratios. The percentages of vehicular emissions and petroleum spills in sediments were much higher than those in water and SPM, indicating the prolonged influence of traffic-related sources. Vehicular emissions, gasoline and diesel fuel leakage on road surface can enter the river through urban runoff, and exhaust from cargo vessels or ferries also strongly contributes to PAHs in the Shanghai river network (Liu et al., 2009). The predominant contributions of traffic-related source and coal and coke combustion to total PAHs in surface sediments of Huangpu river of Shanghai were also found by Liu et al. (2009).

As shown in Fig. 7, the source contributions of total PAHs among different areas varied substantially in SPM and sediments. The biomass combustion, natural gas combustion and vehicular emission sources in island areas were much lower than those in other areas, which was related to the less intensive anthropogenic activities on this island. The source of natural gas showed a high contribution especially in SPM and sediments in the inner city area, showing the influence of intensive use of natural gas for cooking. The contribution of the vehicular emission source was highest in SPM from inner city, followed by industrial areas and suburban towns (Fig. 7b), and was highest in sediments of the inner city area (Fig. 7c). Areas with high population density and high industrial activities are likely to also have higher vehicle numbers. Vehicle emissions in the most urbanized and industrialized areas contributed substantially to PAHs in the river (Kanzari et al., 2014; Liu, A. et al., 2017). In contrast, the total contribution of the six sources in sediments was not high in industrial areas (Fig. 7c), which was mainly attributed to the sediment dredging in some rivers. Since 2006, Shanghai has carried out the "Ten-thousand-river Renovation Plan" in suburban areas. Sediments in many polluted rivers especially in industrial areas and suburban towns have subsequently been dredged, resulting in the much reduced total source contributions in these areas.

4. Conclusions

This study provides quantitative information on the occurrence, spatial distribution and probable sources of PAHs in water, SPM and sediments of the Shanghai river network in China. The levels of PAHs in the river network were low to moderate in comparison with other rivers, but occasional biological toxic effects were apparent in some river sediments. The HMW PAHs represented the major species in sediments and also contributed >50% to total PAHs in water and SPM. The concentrations of PAHs in SPM and sediments varied significantly among the different areas, with the highest concentrations in inner city, characterized by the highly intensive land use and high population density. There was a significant positive correlation between PAH concentrations in sediments and those in SPM and between PAH concentrations in sediments and BC contents. These findings indicated that PAHs in sediments of the Shanghai river network were not only influenced by recent surface runoff, but also by prolonged anthropogenic input. The individual diagnostic ratio and PMF indicated that PAH sources were mainly from a mixture of coal and coke combustion, vehicular emissions, natural gas combustion, petroleum spills and biomass. For both SPM and sediments, the contribution of the vehicular emission source was highest in the inner city area. Vehicle emissions in the most urbanized and industrialized areas contributed strongly to PAHs in the Shanghai river network. We suggest that quantitative parameters such as population density, vehicle number and precipitation should be analyzed to fully interpret PAH variability among different areas.

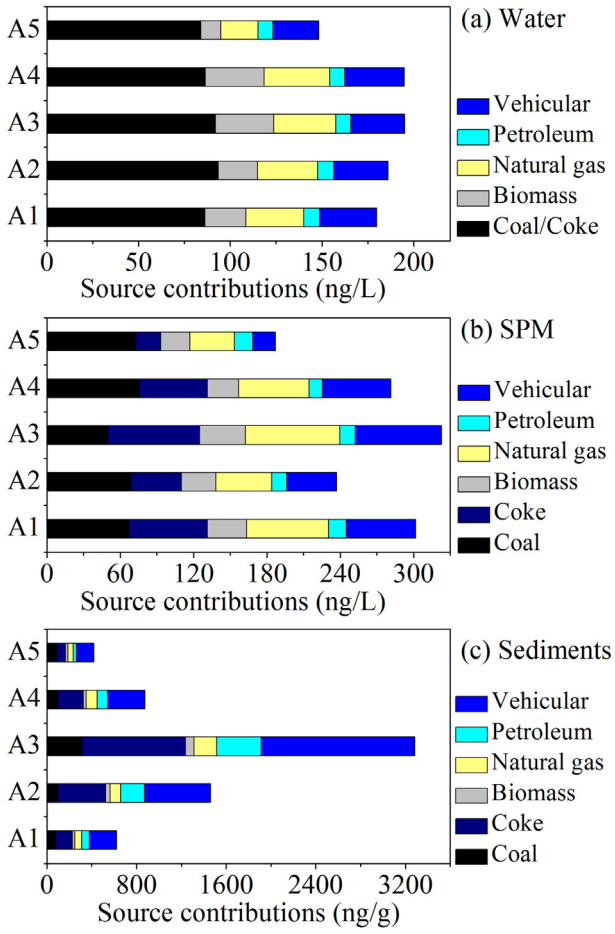

Fig. 7. Contributions of PAHs sources by PMF in in surface water, SPM and sediments of the Shanghai river network. A1, industrial areas; A2, agricultural areas; A3, inner city; A4, suburban towns; A5, island areas.

Acknowledgements

This work was financially supported by the National Natural Science Foundation of China (41271472), the Natural Science Foundation of Shanghai (12ZR1409000), and large instruments and equipment open fund projects of East China Normal University.

References

Chen, Y., Zhu, L., Zhou, R., 2007. Characterization and distribution of polycyclic aromatic hydrocarbon in surface water and sediment from Qiantang River, China. J. Hazard. Mater. 141, 148–155.

Ding, Z.L., Sun, J.M., Liu, T.S., Zhu, R.X., Yang, S.L., Guo, B., 1998. Wind-blown origin of the Pliocene red clay formation in the central Loess Plateau, China. Earth Planet. Sci. Lett. 161, 135–143.

Gelinas, Y., Prentice, K.M., Baldock, J.A., Baldok, J.A., Hedges, J.I., 2001. An improved thermal oxidation method for the quantification of soot/graphitic black carbon in sediments and soils. Environ. Sci. Technol. 35, 3519–3525.

Guo, W., He, M., Yang, Z., Lin, C., Quan, X., Men, B., 2009. Distribution, partitioning and sources of polycyclic aromatic hydrocarbons in Daliao River water system in dry season, China. J. Hazard. Mater. 164, 1379–1385.

Gustafsson, O., Haghseta, F., Chan, C., Macfarlane, J., Gschwend, P.M., 1997. Quantification of the dilute sedimentary soot phase: implications for PAH speciation and bioavailability. Environ. Sci. Technol. 31, 203–209.

Han, J., Bi, C., Chen, Z., Lv, J., Zhou, J., 2012. Pollution characteristics of PAHs in urban runoffs from main roads in urban area. Acta Sci. Circumst. 32, 2461–2469 (in Chinese).

Han, J., Bi, C., Chen, Z., Lv, J., Zhou, J., 2013. Pollution characteristics and source identification of PAHs in urban runoff from different surfaces. Acta Sci. Circumst. 33, 503–510 (in Chinese).

Harrison, R.M., Smith, D.J.T., Luhana, L., 1996. Source apportionment of atmospheric polycyclic aromatic hydrocarbons collected from an urban location in Birmingham, UK. Environ. Sci. Technol. 30, 825–832.

Herngren, L., Goonetilleke, A., Ayoko, G.A., Mostert, M.M.M., 2010. Distribution of polycyclic aromatic hydrocarbons in urban stormwater in Queensland, Australia. Environ. Pollut. 158, 2848–2856.

Kanzari, F., Syakti, A.D., Asia, L., Malleret, L., Piram, A., Mille, G., Doumenq, P., 2014. Distributions and sources of persistent organic pollutants (aliphatic hydrocarbons, PAHs, PCBs and pesticides) in surface sediments of an industrialized urban river (Huveaune), France. Sci. Total Environ. 478, 141–151.

Lee, R.G.M., Coleman, P., Jones, J.L., Lohmann, R., 2005. Emission factors and importance of PCDD/Fs, PCBs, PCNs, PAHs, and PM10 from the domestic burning of coal and wood in the U.K. Environ. Sci. Technol. 39, 1436–1447.

Ligaray, M., Baek, S.S., Kwon, H.-O., Choi, S.-D., Cho, K.H., 2016. Watershed-scale modeling on the fate and transport of polycyclic aromatic hydrocarbons (PAHs). J. Hazard. Mater. 320, 442–457.

Liu, Y., Chen, L., Huang, Q., Li, W., Tang, Y., Zhao, J., 2009. Source apportionment of polycyclic aromatic hydrocarbons (PAHs) in surface sediments of the Huangpu River, Shanghai, China. Sci. Total Environ. 407, 2931–2938.

Liu, Y., Beckingham, B., Ruegner, H., Li, Z., Ma, L., Schwientek, M., Xie, H., Zhao, J., Grathwohl, P., 2013. Comparison of sedimentary PAHs in the rivers of Ammer (Germany) and Liangtan (China): differences between early- and newly- industrialized countries. Environ. Sci. Technol. 47, 701–709.

Liu, S., Liu, X., Liu, M., Yang, B., Cheng, L., Li, Y., Qadeer, A., 2016. Levels, sources and risk assessment of PAHs in multi-phases from urbanized river network system in Shanghai. Environ. Pollut. 219, 555–567.

Liu, A., Duodu, G.O., Mummullage, S., Ayoko, G.A., Goonetilleke, A., 2017. Hierarchy of factors which influence polycyclic aromatic hydrocarbons (PAHs) distribution in river sediments. Environ. Pollut. 223, 81–89.

Liu, H., Lu, D., Song, G., 2017. The development and division of rural township in the suburb of Shanghai metropolitan area were adjusted and studied. Dev. Small Cities Towns 6, 29–34 (in Chinese).

Liu, T., Zhang, Z., Dong, W., Wu, X., Wang, H., 2017. Bioremediation of PAHs contaminated river sediment by an integrated approach with sequential injection of co-substrate and electron acceptor: lab-scale study. Environ. Pollut. 230, 413–421.

Long, E.R., Macdonald, D.D., Smith, S.L., Calder, F.D., 1995. Incidence of adverse biological effects within ranges of chemical concentrations in marine and estuarine sediments. Environ. Manag. 19, 81–97.

Luo, X., Mai, B., Yang, Q., Chen, S., Zeng, E.Y., 2008. Distribution and partition of polycyclic aromatic hydrocarbon in surface water of the Pearl River estuary, South China. Environ. Monit. Assess. 145, 427–436.

Marr, L.C., Kirchstetter, T.W., Harley, R.A., Miguel, A.H., Hering, S.V., Hammond, S.K., 1999. Characterization of polycyclic aromatic hydrocarbons in motor vehicle fuels and exhaust emissions. Environ. Sci. Technol. 33, 3091–3099.

Menzie, C.A., Potokib, B., 1992. Exposure to carcinogenic PAHs in the environment. Environ. Sci. Technol. 26, 1278–1284.

Mitra, S., Bianchi, T.S., 2003. A preliminary assessment of polycyclic aromatic hydrocarbon distributions in the lower Mississippi River and Gulf of Mexico. Mar. Chem. 82, 273–788.

Montuori, P., Aurino, S., Garzonio, F., Sarnacchiaro, P., Nardone, A., Triassi, M., 2016. Distribution, sources and ecological risk assessment of polycyclic aromatic hydrocarbons in water and sediments from Tiber River and estuary, Italy. Sci. Total Environ. 566–567, 1254–1267.

Nelson, D.W., Sommers, L.E., 1982. Total carbon, organic carbon, and organic matter. In: Page, A.L., Miller, R.H., Keeney, D.R. (Eds.), Methods of Soil Analysis, Part 2, Chemical and Microbiological Properties. ASA and SSSA, Madison, pp. 539–579.

Norris, G., Duvall, R., 2014. EPA Positive Matrix Factorization (PMF) 5.0 Fundamentals and User Guide (EPA/600/R-14/108). US EPA.

Ou, D., Liu, M., Xu, S., Cheng, S., Hou, L., Wang, L., 2009. Polycyclic aromatic hydrocarbons partition in particle-water interface in the Yangtze estuarine and nearby coastal areas. Environ. Sci. 30, 1126–1131 (in Chinese).

Sarria-Villa, R., Ocampo-Duque, W., Páez, M., Schuhmacher, M., 2016. Presence of PAHs in water and sediments of the Colombian Cauca River during heavy rain episodes, and implications for risk assessment. Sci. Total Environ. 540, 455–465.

Shen, S.-L., Wu, H.-N., Cui, Y.-J., Yin, Z.-Y., 2014. Long-term settlement behaviour of metro tunnels in the soft deposits of Shanghai. Tunn. Undergr. Sp. Technol. 40, 309–323.

Simcik, M.F., Eisenreich, S.J., Lioy, P.J., 1999. Source apportionment and source/sink relationships of PAHs in the coastal atmosphere of Chicago and Lake Michigan. Atmos. Environ. 33, 5071–5079.

SMSB (Shanghai Municipal Statistics Bureau), 2013. Shanghai Statistical Year Book. China Statistics Press, Beijing, p. 2013.

SMWAB (Shanghai Municipal Water Affairs Bureau), 2016. Shanghai Water Resources Bulletin, Shanghai.

Timoney, K.P., Lee, P., 2011. Polycyclic aromatic hydrocarbons increase in Athabasca River Delta sediment: temporal trends and environmental correlates. Environ. Sci. Technol. 45, 4278–4284.

Uher, E., Mirande-Bret, C., Gourlay-Francé, C., 2016. Assessing the relation between anthropogenic pressure and PAH concentrations in surface water in the Seine River basin using multivariate analysis. Sci. Total Environ. 557–558, 551–561.

Wang, X., Miao, Y., Zhang, Y., Li, Y., Wu, M., Yu, G., 2013. Polycyclic aromatic hydrocarbons (PAHs) in urban soils of the megacity Shanghai: occurrence, source apportionment and potential human health risk. Sci. Total Environ. 447, 80–89.

Yu, W., Liu, R., Xu, F., Shen, Z., 2015. Environmental risk assessments and spatial variations of polycyclic aromatic hydrocarbons in surface sediments in Yangtze River estuary, China. Mar. Pollut. Bull. 100, 507–515.

Yunker, M.B., Macdonald, R.W., Vingarzan, R., Mitchell, R.H., Goyette, D., Sylyestre, S., 2002. PAHs in the Fraser River basin: a critical appraisal of PAH ratios as indicators of PAH source and composition. Org. Geochem. 33, 489–515.

Zhang, S., Zhang, Q., Darisaw, S., Ehie, O., Wang, G., 2007. Simultaneous quantification of polycyclic aromatic hydrocarbons (PAHs), polychlorinated biphenyls (PCBs), and pharmaceuticals and personal care products (PPCPs) in Mississippi river water, in New Orleans, Louisiana, USA. Chemosphere 66, 1057–1069.

Zhang, D., Wang, J., Ni, H., Zeng, H., 2017. Spatial-temporal and multi-media variations of polycyclic aromatic hydrocarbons in a highly urbanized river from South China. Sci. Total Environ. 581–582, 621–628.

Zhao, X., Qiu, H., Zhao, Y., Shen, J., Chen, Z., Chen, J., 2015. Distribution of polycyclic aromatic hydrocarbons in surface water from the upper reach of the Yellow River, northwestern China. Environ. Sci. Pollut. Res. 22, 6950–6956.

Zheng, B., Wang, L., Lei, K., Nan, B., 2016. Distribution and ecological risk assessment of polycyclic aromatic hydrocarbons in water, suspended particulate matter and sediment from Daliao River estuary and the adjacent area, China. Chemosphere 149, 91–100.

Zhu, X., Wang, Y., Liu, W., Zhu, T., 2001. Study on the characteristics of PAHs source profile of coke plant. China Environ. Sci. 21, 266–269 (in Chinese).